

Experimental report

04/06/2021

Proposal: 7-01-562

Council: 4/2021

Title: Band-sticking of phonons at the zone boundary in MnSi

Research area: Physics

This proposal is a new proposal

Main proposer: Tobias WEBER

Experimental team: Tobias WEBER
Michal STEKIEL

Local contacts: Andrea PIOVANO

Samples: MnSi
Cu₂OSeO₃

Instrument	Requested days	Allocated days	From	To
IN8	4	3	21/05/2021	25/05/2021
IN3	2	2	11/05/2021	14/05/2021

Abstract:

Non-symmorphic symmetry in combination with time-reversal symmetry conspire to act effectively as a mirror symmetry that is predicted to generate so-called generic sticking of the band structure of crystals, i.e., degenerate crossing points where band gaps would be expected. We propose to search for band-sticking in the phonon-spectrum of MnSi at the Brillouin zone boundary, where we recently observed related band sticking in the electronic bands. Evidence for the phonon-band sticking would establish the generic origin of the band-sticking in the electronic structure and, at the same time provide a new perspective of the properties of a wide range of isostructural siblings such as FeSi or CoSi, crystallizing in the P213 space group. In total we ask for four days of beamtime at IN8.

Band-sticking of magnons at the zone boundary of a chiral magnet

T. Weber,^{1,*} M. Stekiel,² A. Piovano,¹ A. P. Schnyder,³ M. A. Wilde,² and C. Pfleiderer²

¹*Institut Laue-Langevin (ILL), 71 avenue des Martyrs, 38000 Grenoble, France*

²*Physik-Department E21, Technische Universität München (TUM), James-Frank-Str. 1, 85748 Garching, Germany*

³*Max-Planck-Institut für Festkörperforschung, Heisenbergstr. 1, D-70569 Stuttgart, Germany*

(Dated: June 4, 2021)

The lack of an inversion symmetry for compounds crystallising in the $P2_13$ space group has led to the theoretical prediction of energetic degeneracies in their electron and magnon band structures, a so-called “band-sticking” [1]. This effect has been predicted to be centred around the corner $R = (0.5 \ 0.5 \ 0.5)$ of the cubic Brillouin zone [1]. Performing de Haas-van Alphen measurements of the magnetisation, Wilde *et al.* very recently confirmed the appearance of electronic band degeneracies around the R point of the chiral magnet $MnSi$ [2]. They could influence and lift these degeneracies by changing the angle of the applied external magnetic field.

For the present experiment, we investigated the magnon dispersion branches around the cubic R point in single-crystalline Cu_2OSeO_3 using the IN8 spectrometer [3]. This compound was chosen over $MnSi$ because for the latter the R point would lie in the Stoner continuum of non-collective single-particle excitations [4], see also our experimental report #4-01-1734. Cu_2OSeO_3 shares similar magnetic phases as $MnSi$, including a skyrmion phase, and its magnons had already been comprehensively mapped out in zero external field [5], allowing us to focus on their detail measurements.

The Cu_2OSeO_3 single-crystal was cooled to $T = 10$ K and the bulk of the experiment was performed around its (440) Bragg reflection. (440) was chosen for its large nuclear structure factor and its wave vector being low enough for a sufficiently strong magnetic form factor. The crystal was oriented in the (hhl) plane, and we applied a horizontal field of magnitude $B = 0.2$ T in two scan series along the [001] and [110] directions, respectively, using an Oxford cryomagnet [6]. Auxiliary measurements were done around the (222) Bragg peak,

with an additional field orientation along the [111] direction. The pure nuclear signal including the phonons was measured in a separate scan series outside the magnetic phases, at $T = 80$ K.

Figures 1 and 2 show two of our main scan series. The high- T phonon scans (blue data points) were scaled to the intensities of the magnon scans using the ratio of the respective Bose factors. Furthermore, the magnon scans for the two different field directions were also scaled so that their background intensities coincide. This was necessary because of a weaker signal for one of the field direction due to variations in the crystal tilt and different attenuation effects caused by the magnet.

We observe profound effects on the magnons when changing the field direction from [001] (black data points) to [110] (red data points). For example, at the R point with its reduced wave-vectors of $q = (0.5 \ 0.5 \ 0.5)$ (right bottom panel of Figure 1) the strong magnon at ca. $E = 8.5$ meV, which appears for $B \parallel [110]$, is absent for $B \parallel [001]$, while magnon at ca. 10 meV remains unchanged for both field directions. Note that the signal at ca. 7 meV is a phonon, as can be observed in the $T = 80$ K control scan (blue data points).

Our results are very promising and a thorough theoretical analysis is in order to decipher the observed effects. For future experiments, we both plan to perform a longitudinal polarisation analysis at IN20 or IN22 to disentangle the phonon and magnon spectra, as well as finer measurements of the R point magnon at a lower instrumental final energy E_f and thus better resolution at Thales or IN12.

Data DOI: [10.5291/ILL-DATA.7-01-562](https://doi.org/10.5291/ILL-DATA.7-01-562).

-
- [1] T. Jeong and W. E. Pickett, *Phys. Rev. B* **70**, 075114 (2004).
[2] M. A. Wilde, M. Dodenhöft, A. Niedermayr, A. Bauer, M. M. Hirschmann, K. Alpin, A. P. Schnyder, , and C. Pfleiderer, “Symmetry-enforced topological nodal planes at the fermi surface of a magnet,” (2021), in review.
[3] A. Hiess, M. Jiménez-Ruiz, P. Courtois, R. Currat, J. Kulda, and F. Bermejo, *Physica B: Condensed Matter* **385-386**, 1077 (2006).
[4] Y. Ishikawa, G. Shirane, J. A. Tarvin, and M. Kohgi,

Phys. Rev. B **16**, 4956 (1977).

- [5] P. Y. Portnichenko, J. Romhányi, Y. A. Onykienko, A. Henschel, M. Schmidt, A. S. Cameron, M. A. Surmach, J. A. Lim, J. T. Park, A. Schneidewind, D. L. Abernathy, H. Rosner, J. van den Brink, and D. S. Inosov, *Nature communications* **7**, 1 (2016).
[6] ILL Sample Environment, “Oxford 3.8 T cryomagnet 134OXHV38,” .

* Correspondence: tweber@ill.fr

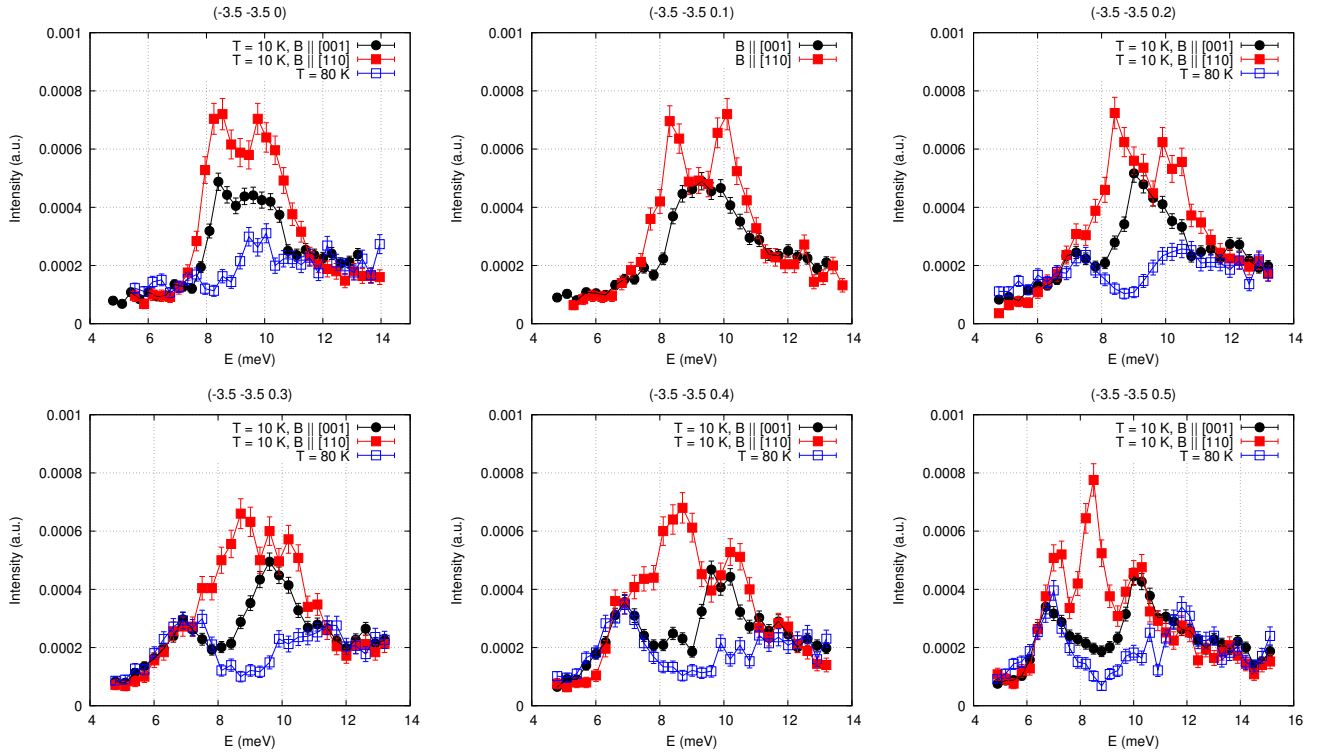


Figure 1. Path along the cubic zone boundary from $q_i = (0.5 \ 0.5 \ 0)$ (left top) to $q_f = (0.5 \ 0.5 \ 0.5)$ (right bottom). The black and red points depict scans with field $B \parallel [001]$ and $B \parallel [110]$, respectively. The blue points are control measurements outside the magnetic phases. Note that for better comparison, the data have been scaled in intensity so that their backgrounds coincide.

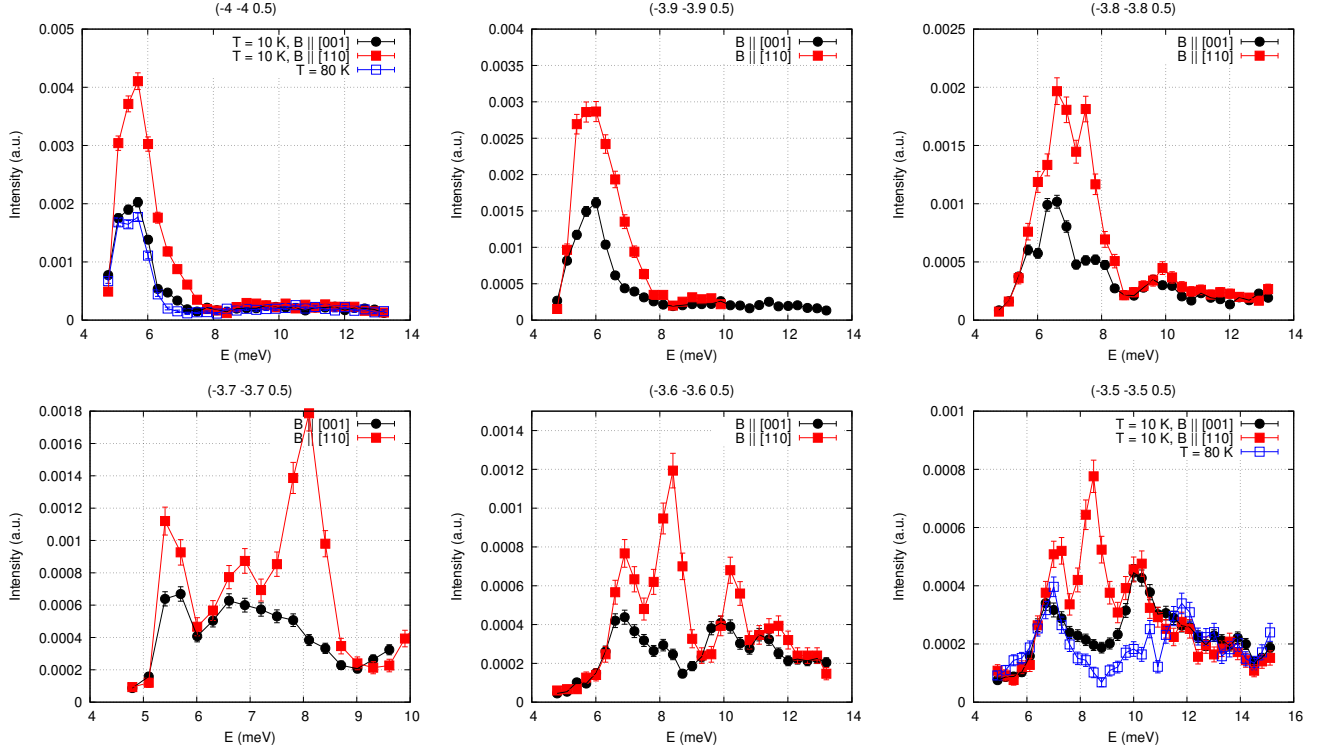


Figure 2. Path along the cubic zone boundary from $q_i = (0 \ 0 \ 0.5)$ (left top) to $q_f = (0.5 \ 0.5 \ 0.5)$ (right bottom). The black and red points depict scans with field $B \parallel [001]$ and $B \parallel [110]$, respectively. The blue points are control measurements outside the magnetic phases. Note that for better comparison, the data have been scaled in intensity so that their backgrounds coincide.